Geometric synthesis and kinematic analysis of a combined double-wedging mechanism of the pressure plate drive in the die-cutting press

ABSTRACT

The analysis of existing publications highlights a gap in scientific research on mechanisms used in the drive system to move the pressure plate, particularly those that extend the contact duration between the die-cutting mold and cardboard. The authors developed a kinematic scheme of the proposed double-wedging mechanism. The geometric synthesis and kinematic analysis of the mechanism were performed, determining the relative values of key geometric parameters, displacement, velocity, and acceleration of the pressure plate. The geometry and kinematic parameters were calculated using mathematical models based on similarity invariants. To validate the results, a simulation of the work process was conducted in the SolidWorks program for the double-wedging mechanism and the existing mechanism used in Bobst presses. A comparative analysis of the analytically obtained kinematic dependencies and the simulation results demonstrated absolute agreement, confirming the accuracy of the developed mathematical models. The results of the kinematic analysis indicate that using a combined two-wedging mechanism doubles the duration of the die-cutting tool with the cardboard blank. This prolonged contact positively impacts the efficiency of die-cutting operations, particularly for creasing and relief embossing.

Vitalii Vlakh (1) Ivan Rehei ¹ (1) Oleh Knysh ¹ (1)

¹ Lviv Polytechnic National University, Lviv, Ukraine

Corresponding author: Vitalii Vlakh e-mail: vlakh.v.v@gmail.com

First received: 24.11.2024. Revised: 3.3.2025. Accepted: 10.3.2025.

KEY WORDS

die-cutting press, cardboard blank, double-wedging mechanism, crank, pressure plate, analysis

Introduction

Die-cutting of cardboard blanks is the primary method for manufacturing packaging. Using a flat die-cutting mold, operations such as cutting, creasing, and cold embossing of sheet cardboard blanks are carried out (Fig. 1). Flat die-cutting molds allow the production of cardboard packaging in various sizes and shapes (Emblem & Emblem, 2012).

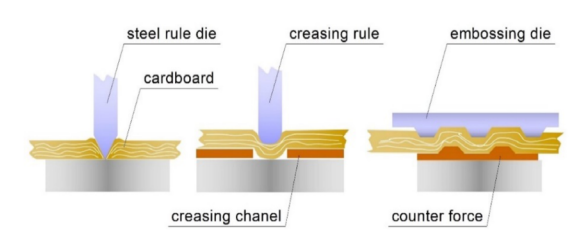
The mold consists of steel cutting and creasing rules embedded in a laser-cut plywood base. The pressure plate contains creasing and embossing matrices for pressing. Ejector elements facilitate the removal of die-cut blanks from the blades.

Paper and cardboard packaging are widely used due to their recyclability, durability, aesthetic appeal, and versatility. Ensuring high quality in production requires precise technological processes (Kirwan, 2013).

The manufacturing process of cardboard containers involves several automated technological operations. The chain of technological operations is carried out automatically during stops of the cardboard blank using transportation in the equipment sections (Rehei, 2011).

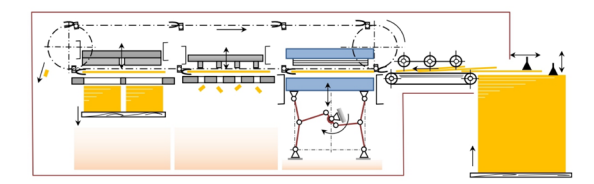
Modern die-cutting equipment is built according to the sectional principle. As an example, the BOBST multi-section die-cutting machine (Fig. 2) consists of the following units:

- cardboard blank feeding and stacking section
- die-cutting press section
- scrap removal section
- separation and stacking section



» **Figure 1:** Tools of the press pair of the die-cutting operation of sweeps for cutting, creasing, and cold embossing

The movement of semi-finished products between sections is performed by carriages attached to chain conveyors. The die-cutting press section is particularly critical as it utilizes wedging mechanisms to drive the pressure plate.



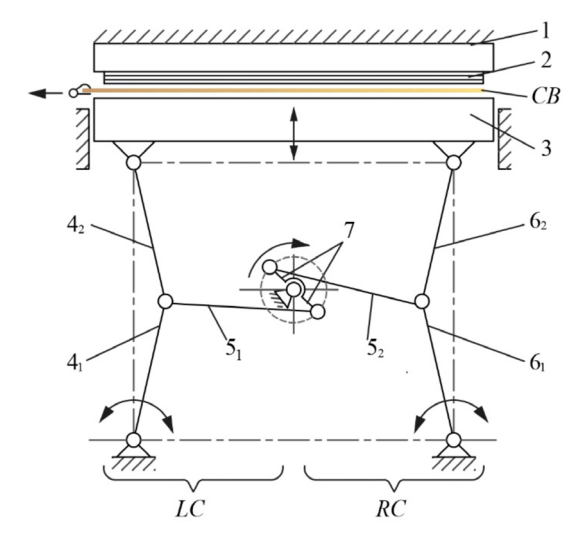
» Figure 2: Scheme of a multi-section die-cutting machine

The operation principle of BOBST die-cutting presses has been successfully implemented in such models as AUTOPLATEN, EXPERTCUT, and MASTERCUT. In these machines, a flat die-cutting mold 2 is fixed on the upper stationary plate 1 (Fig. 3). The pressure on the workpiece $\it CB$ is created by the pressure plate 3, which receives reciprocating motion along the guides from the two-circuit lever mechanism of second-class. Hinges connect the two-armed crank 7, to which connecting rods $\it 5_1$ and $\it 5_2$ transmit motion to driving rods $\it 4_1$ and $\it 6_2$. Connecting rods $\it 4_2$ and $\it 6_2$ are connected to driving rods, which transmit motion to plate 3.

The mechanism's construction involves the mutual arrangement of lever pairs 4_1 , 4_2 , and 6_1 , 6_2 in the uppermost pressure plate position 3, ensuring that the angle between them approaches 180°. This configuration enables the attainment of the "wedging effect"- the significant technological efforts developed by the pressure plate at the moment of contact with the cardboard blank.

Rehei et al. (2022) analyzed four existing drive mechanisms, among which are mechanisms used in the die-cutting equipment of the BOBST and Heidelberg companies. According to the analytical analysis results, the pressure plate's acceleration in the existing wedging mechanism

(BOBST) reaches its maximum value at the moment it contacts the die-cutting mold.



» **Figure 3:** The kinematic scheme of the existing wedging mechanisms of the pressure plate drive

Khvedehyn & Zelenyi (2014) analyzed the existing structures of the pressure plate drive mechanisms in die-cutting equipment. As the authors note, their design causes asymmetry of the right and left parts of the pressure plate during motion. The symmetry of the plate movement is observed only at the final stage of its movement: the working surface of the pressure plate becomes parallel to the support plate surface during the cutting and creasing of cardboard blanks. Such asymmetry causes uneven load distribution and generates pressure plate oscillations in the press, which reduces its operation efficiency. Analytical studies of various pressure plate drive mechanisms allow us to assess their efficiency. In their research work Kuznetsov, Kolomiets & Dimitraschuk (2012) conducted analytical studies of a flat die-cutting press with an existing wedging mechanism in the pressure plate drive. Analytical studies proved the presence of uneven movement during the cycle of movement of the pressure plate.

Lin, Zhou & Huang (2015) also studied a die-cutting press with a wedging mechanism. The analysis carried out by the authors showed high values of the pressure plate's inertia force during its motion. That has a significant impact on the drive mechanism of the die-cutting press and its kinematic accuracy. It is essential that when the maximum acceleration is reached, a shock load will occur. Considering the shortcomings, the authors proposed an optimized pressure plate drive mechanism. The main goal of implementing the proposed mechanism is to improve the characteristics of the pressure plate movement. A cam mechanism is presented in the drive of the pressure plate. However, the design of this mechanism is complicated due to the production of drive cams with two contact profiles.

In addition, such drive cams are dimensional. Shakhbazov et al. (2020) proposed a new design of wedging cam mechanisms to drive the pressure plate in die-cutting presses. The authors conducted theoretical calculations of technological loads that occur during the cutting and creasing of cardboard blanks.

The authors also investigated the driving forces arising in the proposed lever-cam mechanism. Despite some design simplification, the mechanism still needs to be improved to be set up and operated. In addition, the authors did not conduct experimental studies of the proposed mechanism.

Authors Pasika & Vlakh (2016) developed a methodology for optimizing the central shaft functioning of the wedging mechanism. It makes it possible to increase the efficiency of die-cutting presses, provided that its energy consumption is reduced. The authors obtained analytical dependencies for the synthesis of the mechanism. The authors suggested using a two-armed crank on the main shaft with a defined swing angle, calculated based on the synthesis results, to avoid uneven pressure plate movement. Vlakh & Pasika (2016) also suggested installing an additional four-link or rocker mechanism in the drive to improve the quality of die-cutting cardboard blanks.

However, using additional mechanisms as part of the drive complicates the design and adjustment of die-cutting presses. Kuznetsov, Rehei & Vlakh (2017) proposed using a two-slider combined mechanism to eliminate the disadvantages associated with uneven movement of the pressure plate and reduce the press's dimensions. The proposed mechanism consists of two crank-slider circuits: drive and driven. Using this mechanism reduces the overall load and peak kinetic energy consumption.

However, in addition to the significant advantages of the proposed mechanism, it creates much less effort during the die-cutting process than the existing wedging mechanism.

In the research work of Wang, Chen & Li (2023) experimental studies of the existing press with a wedging mechanism of the pressure plate drive were carried out. The press, loaded with the maximum technological die-cutting resistance of 350 tons under the condition of the rotation frequency of the main shaft of 125 rpm, was studied. An engineering decision changed the design of the drive rod, leading to a significant reduction in pressure plate oscillation.

To solve problems related to the shortcomings of the design of the existing mechanism and the task of increasing the duration of contact of the die-cutting tool with the cardboard blank, Rehei et al. (2023) proposed using a gear with an additional driven crank in the driven circuit of the wedging mechanism.

The design of the proposed mechanism, where the driven crank is in the lower initial position, has a positive effect on the creasing and embossing operations of the cardboard. Such a construction of the mechanism should eliminate the operational shortcomings associated with the oscillation of the pressure plate during the mechanism's kinematic cycle. In such a mechanism, the plate approaches more slowly. It is placed parallel to the stationary plate even before the technological operation is performed, and the oscillating movement does not affect the quality of die-cutting cardboard sweeps.

There is no information in the scientific information space on the research of the mechanisms of the movement of the pressure plate with an increased duration of contact of the die-cutting tools with the cardboard. Scientific research in this direction is essential and actual.

The work aims to synthesize and evaluate the quantitative and qualitative characteristics of the kinematic parameters of the double-wedging mechanism in the pressure plate drive of the die-cutting press.

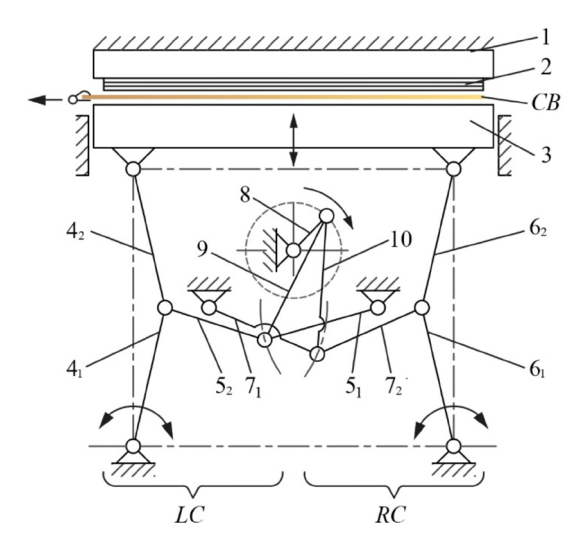
The following tasks must be solved to achieve the goal:

- to conduct a critical analysis of scientific research in the direction of improving die-cutting presses and formulate the goal and objectives of the study
- to develop a kinematic scheme of the double wedging mechanism of the pressure plate drive of the die-cutting press
- to perform a geometric synthesis of the proposed mechanism
- to develop a methodology for calculating the kinematic parameters of the proposed combined double-wedging mechanism
- to calculate the relative kinematic parameters of the proposed combined double-wedging mechanism of the pressure plate drive
- to conduct a virtual experiment of the mechanism and investigate its kinematic parameters in the SolidWorks software (Dassault Systèmes, France)
- to perform a comparative analysis of the analytical studies' results with the results of a virtual experiment of the existing and proposed double-wedging mechanisms in the SolidWorks program

The press of the die-cutting machine proposed by the authors consists of an upper stationary plate 1 (Fig. 4), fixed to the base, with a flat die-cutting mold 2; movable pressure plate 3; a set of wedging mechanisms of the left circuit LC: lever 4_1 and connecting rod 4_2 of the vertical wedging circuit, lever 5_1 and connecting rod 5_2 of the horizontal wedging circuit; a set of wedging circuits of the right circuit RC: lever 6_1 and connecting rod 6_2 of the vertical wedging mechanism, lever 7_1 and connecting rod 7_2 of the horizontal wedging circuit; crank 8; left 9 and right 10 connecting rods of the driving wedging circuits.

The press of the die-cutting machine works as follows. In the initial position, pressure plate 3 is in the lower position, and the cardboard blank is in the die-cutting zone. When turning the crank 8 clockwise, left 9 and right 10 connecting rods wedge the horizontal circuits by aligning lever 5_1 and connecting rod 5_2 of the left circuit LC and lever 7_1 and connecting rod 7_2 of the right circuit RC.

As a result of this action, the vertical circuits are wedged by aligning lever 4_1 and connecting rod 4_2 of the left circuit LC and lever 6_1 and connecting rod 6_2 of the right circuit RC, which ensures the lifting of the pressure plate 3 and die-cutting the sweeps with tools of mold 2 in its upper position. Further crank rotation clockwise 8 leads to decreased angles between the links of all wedging circuits. This causes pressure plate 3 to be lowered to remove the die-cut cardboard blank CB and feed it into the die-cutting zone.



» Figure 4: The kinematic scheme of the double-wedging drive mechanism of the die-cutting press

Methods, CAD/CAE Analysis

Geometric Synthesis of the Mechanism

Two identical combined mechanisms of the left *LC* and right *RC* circuits drive the pressure plate. The geometric synthesis and kinematic analysis focus on a single contour, specifically the left circuit.

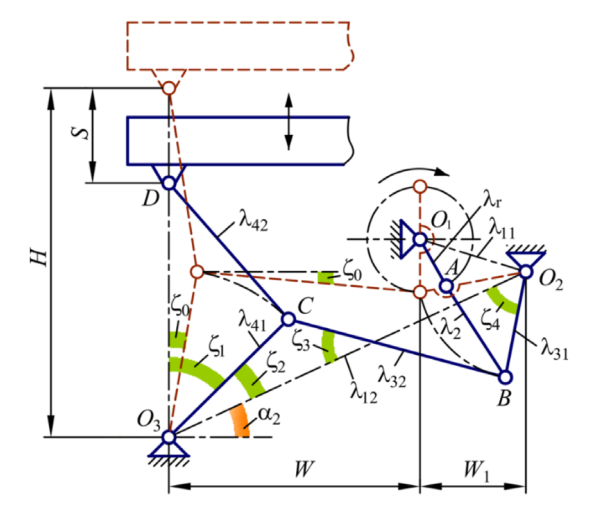
Relative and absolute parameters were defined to calculate the kinematic characteristics of the double-wedging mechanism's left contour.

The values are obtained from the proportion of the actual die-cutting press dimensions:

- S = 1 maximum linear displacement of the pressure plate (Fig. 5)
- W = 3.125 horizontal distance between supports O₁ and O₃ of the wedging mechanism of the left circuit
- W₁ = 1.5625 horizontal distance between supports O₁ and O₂ of the wedging mechanism of the left circuit
- H = 6.25 total height of the mechanism

Designation of absolute parameters:

- ϕ angle of rotation of the driving crank
- γ_0 = 5° restriction angle of wedging contours to avoid "jamming" of the mechanism



» Figure 5: Scheme for calculating the left contour of the double-wedging mechanism of the pressure plate drive (determination of links and extreme position angles of the driving and driven contours)

For the kinematic calculation of the mechanism, its main relative geometric parameters are determined based on the conducted synthesis:

- λ_r the driving crank size (Fig. 5)
- λ_{11} the interbase distance between axes O_1 and O_2
- λ_{12} the interbase distance between axes O_3 and O_2
- λ_2 the connecting rod length of the driving circuit
- $\lambda_{_{31}}$ the lever length of the horizontal wedging circuit
- λ_{32} the power rod length of the horizontal wedging circuit
- $\lambda_{_{\!41}}$ the lever length of the vertical wedging circuit
- $\lambda_{_{42}}$ the connecting rod length of the vertical wedging circuit

Mathematical models using similarity invariants were developed to determine the rational design parameters and ensure optimal mechanism operation. Equations were formulated to calculate angles, distances, and link lengths, establishing a foundation for further kinematic analysis. All equations were derived by the authors during the project's work.

The well-known method of calculating initial and combined mechanisms involves using a "single" mechanism (Poliudov, 2005). The driving crank is assumed to be equal to one ($O_1A = 1$, Fig. 5). The synthesis of the double-wedging mechanism of the pressure plate drive developed in this paper involves a "reverse" calculation. Here, the "unit" is the relative linear movement S = 1 of the driven link- the pressure plate, corresponding to its movement ($S_{max} = 80$ mm, 3.14961 in) in the BOBST die-cutting presses.

The primary geometric parameters were defined according to the following geometric dependencies to carry out a geometric synthesis of the researched mechanism.

The angle of inclination α_2 of the interbase distance λ_{12} to the vertical axis:

$$\alpha_2 = \arctan\left(\frac{H}{2 \cdot (W + W_1)}\right)$$

The relative length of the drive rod λ_{41} of the driven circuit and the connecting rod length λ_{42} of the driven circuit ($\lambda_{42} = \lambda_{41}$):

$$\lambda_{42} = H \cdot \frac{\sin(\xi_0)}{\sin(\pi - 2 \cdot \xi_0)}$$

The angle of inclination ξ_1 to the vertical of the drive rod λ_{a_1} in the mechanism's lowermost position:

$$\xi_1 = \arccos\left(\frac{(H-S)^2}{2 \cdot \lambda_{42} \cdot (H-S)}\right)$$

The relative length of the power rod λ_{32} of the driven circuit:

$$\lambda_{32} = \frac{W - \lambda_{42} \cdot \sin(\xi_0)}{\cos(\xi_0)}$$

The relative length of the driven rod $\lambda_{_{31}}$ of the driving circuit:

$$\lambda_{31} = \sqrt{(\lambda_{32} \cdot \sin(\xi_0))^2 + W_1^2}$$
 (5)

The inclination angle $\xi_{_2}$ of the interbase distance $\lambda_{_{12}}$ to the vertical axis:

$$\xi_2 = \frac{\pi}{2} - \xi_1 - \alpha_2 \tag{6}$$

The relative length of the interbase distance λ_{ij} between the O₂ and O₃ axes:

$$\lambda_{12} = \sqrt{(W + W_1)^2 \cdot (\frac{H}{2})^2}$$
 (7)

It is necessary to solve the equations system to determine the angles ξ_3 and ξ_4 and further calculate the mechanism's main parameters:

$$\begin{cases} A\cos\xi_2 + B\cos\xi_3 + C\cos\xi_4 = D \\ A\sin\xi_2 + C\sin\xi_4 = B\sin\xi_3 \end{cases}$$
 (8)

where A=
$$\lambda_{41}$$
, B= λ_{32} , C= λ_{31} , D= λ_{12} > 0; ξ_{2} , ξ_{32} , ξ_{4} are (0; π /2).

Reducing the equations system (8) to the form:

$$\begin{cases}
B\cos\xi_3 + C\cos\xi_4 = D - A\cos\xi_2 \\
-B\sin\xi_3 + C\sin\xi_4 = -A\sin\xi_2
\end{cases} \tag{9}$$

Reducing the equations system (9) to a new form:

$$\begin{cases} B\cos\xi_3 + C\cos\xi_4 = K \\ -B\sin\xi_3 + C\sin\xi_4 = L \end{cases} \tag{10}$$

where K=D-A·cosξ2, L=-A·sinξ2.

(1) Expressing from the first equations system (10) $\cos \xi 3$:

$$\cos \xi_3 = \frac{K}{B} - \frac{C}{B} \cos \xi_4 \tag{11}$$

Considering the ratio between the trigonometric functions of the same argument:

$$\sin \xi_3 = \sqrt{1 - \left(\frac{K}{B} - \frac{C}{B}\cos \xi_4\right)^2} \tag{12}$$

Substituting the expression (12) into the second equation of system (10):

$$-B\sqrt{1-\left(\frac{K}{B}-\frac{C}{B}cos\xi_4\right)^2}+Csin\xi_4=L\tag{13}$$

or

(2)

(3)

$$\sqrt{1 - \left(\frac{K}{B} - \frac{C}{B}\cos\xi_4\right)^2} = \frac{C}{B}\sin\xi_4 - \frac{L}{B}.$$
 (13)

Squaring both parts of equation (13):

$$1 - \left(\frac{K}{B} - \frac{C}{B}\cos\xi_4\right)^2 = \left(\frac{C}{B}\sin\xi_4 - \frac{L}{B}\right)^2 \tag{14}$$

After transformations (14), we got:

$$K\cos\xi_4 + L\sin\xi_4 = \frac{K^2 + C^2 + L^2 - B^2}{2C}$$
 (15)

Entering the value $\frac{K^2 + C^2 + L^2 - B^2}{2C} = \tilde{L}$, dependence (15) takes the form:

$$K\cos\xi_4 + L\sin\xi_4 = \widetilde{L}$$
 (16)

Using the ratio between trigonometric functions of the same argument, we got:

$$K\sqrt{1-\sin^2\xi_4} + L\sin\xi_4 = \widetilde{L} \tag{17}$$

or

$$K\sqrt{1-\sin^2\xi_4} = \widetilde{L} - L\sin\xi_4 \tag{17}$$

Squaring both parts of equation (17):

$$(K^2 + L^2)\sin^2\xi_4 - 2L\cdot \tilde{L}\sin\xi_4 + (\tilde{L}^2 - K^2) = 0$$
 (18)

A quadratic equation relative to $\sin \xi_4$ was obtained. The roots of the quadratic equation (18):

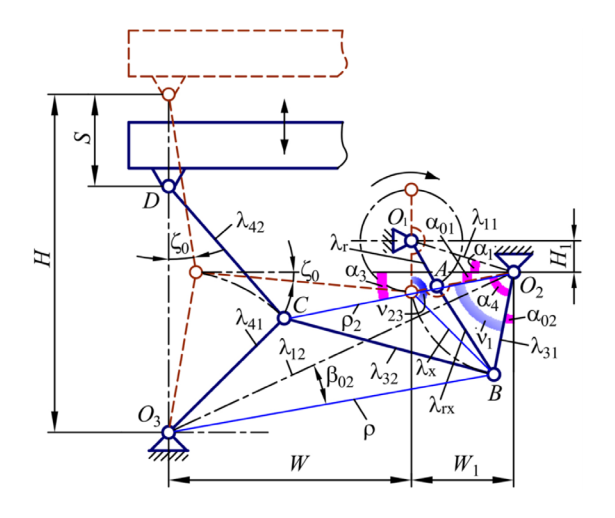
$$\xi_{4} = arcsin\left(\frac{2L\cdot\widetilde{L} \pm \sqrt{\widetilde{D}}}{2(K^{2} + L^{2})}\right)$$
 (19)

where $\widetilde{D} = (2L \cdot \widetilde{L})^2 - 4(K^2 + L^2)(\widetilde{L}^2 - K^2)$ – discriminant

Substituting (19) into the second equation of system (10), we got:

$$\xi_3 = \arcsin\left(\frac{C\left(2L\cdot\widetilde{L} \pm \sqrt{\widetilde{D}}\right)}{2B\left(K^2 + L^2\right)} - \frac{L}{B}\right) \tag{20}$$

Calculating the following geometric parameters shown in Fig. 6 is necessary to determine the dimensions of crank $\lambda_{\rm R}$ and the connecting rod $\lambda_{\rm S}$.



» Figure 6: Scheme for calculating the left contour of the double-wedging mechanism of the pressure plate drive (determining the dimensions of the crank and the driving connecting rod)

The relative length ρ of the straight line from support O_2 to the lowermost position of the kinematic pair B:

$$\rho = \sqrt{\lambda_{12}^2 + \lambda_{31}^2 - 2 \cdot \lambda_{12} \cdot \lambda_{31} \cdot \cos(\xi_4)}$$
 (21)

The angle β_{02} between the straight line ρ and the interbase distance λ_{12} :

$$\beta_{02} = \arccos(\frac{\lambda_{12}^2 + \rho^2 - \lambda_{31}^2}{2 \cdot \lambda_{12} \cdot \rho})$$
 (22)

The angle α_{01} between the central horizontal axis and the driven rod λ_{31} in the uppermost position of the mechanism:

$$\alpha_{01} = \arccos[iii](\frac{\lambda_{31}^2 + W_1^2 - (\lambda_{32} \cdot \sin(\xi_0))^2}{2 \cdot \lambda_{31} \cdot W_1})$$
 (23)

The inclination angle α_{o2} of the driven rod λ_{31} to the vertical axis in the lowest position of the mechanism:

$$\begin{array}{l} \alpha_{02} = \arccos \\ \\ \left(\frac{\lambda_{31}^2 + \frac{H^2}{4} - \rho^2 - (W + W_1)^2 + 2 \cdot \rho \cdot (W + W_1) \cdot \cos(\alpha_2 - \beta_{02})}{2 \cdot \lambda_{31} \cdot \frac{H}{2}} \right) \end{array}$$

Swing angle v_1 of the driven rod λ_{31} :

$$v_1 = \frac{\pi}{2} - \alpha_{01} - \alpha_{02} \tag{25}$$

The relative length λ_x between the extreme positions of the kinematic pair B:

$$\lambda_{X} = \sqrt{2 \cdot \lambda_{31}^{2} (1 - \cos(\nu_{1}))}$$
 (26)

Angle $O_1B_1B_2 V_{23}$:

$$v_{23} = \frac{\pi - v_1}{2} + \arctan\left(\frac{W_1}{\lambda_{32} \cdot \sin\left(\xi_0\right)}\right) \tag{27}$$

The relative length of the driving crank λ :

$$\lambda_r = \frac{\lambda_X \cdot \sqrt{\cos(\nu_{23})^2 + 8} - \cos(\nu_{23})}{8}$$
 (28)

The relative vertical distance H₁ between supports O₁ and O₂:

$$H_1 = \lambda_r - \lambda_{32} \cdot \sin(\xi_0) \tag{29}$$

The relative interbase distance λ_{11} between supports O₁ and O₂:

$$\lambda_{11} = \sqrt{W_1^2 + H_1^2} \tag{30}$$

The angle α_1 of inclination of the interbase distance to the horizontal axis:

$$\alpha_1 = \arctan\left(\frac{H_1}{W_1}\right) \tag{31}$$

The relative length of the straight line ρ_2 between the uppermost position of the kinematic pair C and the support O₂:

$$\rho_2 = \sqrt{\lambda_{42}^2 + \lambda_{12}^2 - 2 \cdot \lambda_{42} \cdot \lambda_{12} \cdot \cos(\xi_2)}$$
 (32)

The angle α_3 between the straight line ρ_3 and the horizontal axis:

$$\alpha_3 = \arccos$$

$$\left(\frac{(W + W_1 - \lambda_{42} \cdot \sin(\xi_0))^2 + \rho_2^2 - 2 \cdot \lambda_{42}^2 \cdot (1 - \cos(\xi_1 - \xi_0))}{2 \cdot (W + W_1 - \lambda_{42} \cdot \sin(\xi_0)) \cdot \rho_2}\right)$$

(33)

The angle $\alpha_{_4}$ between the straight line $\rho_{_2}$ and the driven rod $\lambda_{_{31}}$, which is in the lowest position:

$$\alpha_4 = \arccos\left(\frac{\rho_2^2 + \lambda_{31}^2 - \lambda_{32}^2)}{2 \cdot \rho_2 \cdot \lambda_{31}}\right) \tag{34}$$

The relative length λ_{rx} of the straight line between support O, and kinematic pair B in the lowest position:

$$r_x = \sqrt{\lambda_{11}^2 + \lambda_{31}^2 - 2 \cdot \lambda_{31} \cdot \lambda_{11} \cdot \cos[iii]} (\alpha_1 + \alpha_3 + \alpha_4).$$
 (35)

The relative size of the connecting rod λ , of the driving circuit:

$$\lambda_2 = {}_{rx} - \lambda_r \tag{36}$$

Kinematic Calculation of the Mechanism

The kinematic parameters are initially calculated by determining the end position of the four-link mechanism O₁ABO₂. Figure 7 shows the mechanism link position angles, and the analytical dependencies for their calculation are given below.

The angle φ_0 between the initial position of the driving crank λ_r and the base distance λ_n :

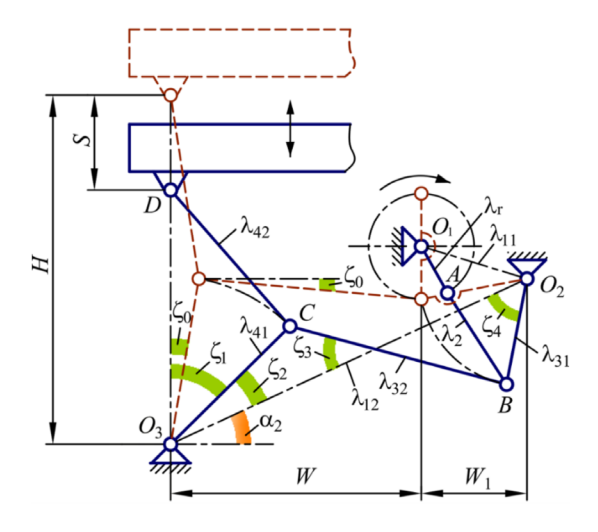
$$\varphi_0 = \arccos\left(\frac{(\lambda_r + \lambda_2)^2 + \lambda_{11}^2 - \lambda_{31}^2)}{2 \cdot (\lambda_r + \lambda_2) \cdot \lambda_{11}}\right)$$
(37)

The angle φ_{01} between the initial position of the driving crank λ_r and the vertical axis:

$$\varphi_{01} = \arccos\left(\frac{(\lambda_2 - \lambda_r)^2 + \lambda_{11}^2 - \lambda_{31}^2)}{2 \cdot (\lambda_2 - \lambda_r) \cdot \lambda_{11}}\right)$$
(38)

Angle ϕ_{max} :

$$\varphi_{max} = \pi + \varphi_0 + \varphi_{01} \tag{39}$$



» Figure 7: Scheme for calculating the left contour of the double-wedging mechanism of the pressure plate drive (determination of the angles of the extreme position of the four-link mechanism and the driving crank)

Angles γ_{01} and γ_{0} between the lowermost position of the driven rod λ_{31} and the interbase distance λ_{11} :

$$\gamma_{01} = \arccos\left(\frac{\lambda_{11}^{2} + \lambda_{31}^{2} - (\lambda_{r} + \lambda_{2})^{2}}{2 \cdot \lambda_{11} \cdot \lambda_{31}}\right)$$
(40)

$$\gamma_0 = \pi - \gamma_{01} \tag{41}$$

The angle γ_{02} between the uppermost position of the driven rod λ_{31} and the interbase distance λ_{31} :

$$\gamma_{02} = \arccos\left(\frac{\lambda_{31}^2 + \lambda_{11}^2 - (\lambda_2 - \lambda_r)^2)}{2 \cdot \lambda_{11} \cdot \lambda_{31}}\right)$$
(42)

Swing angle γ_{max} of the driven rod $\lambda_{_{\! 31}}\!\!:$

$$\gamma_{max} = \pi - \gamma_{02} \tag{43}$$

The following calculation stage determines the mechanism's current position. Figure 8 shows the necessary parameters for this calculation.

The relative diagonal Δ :

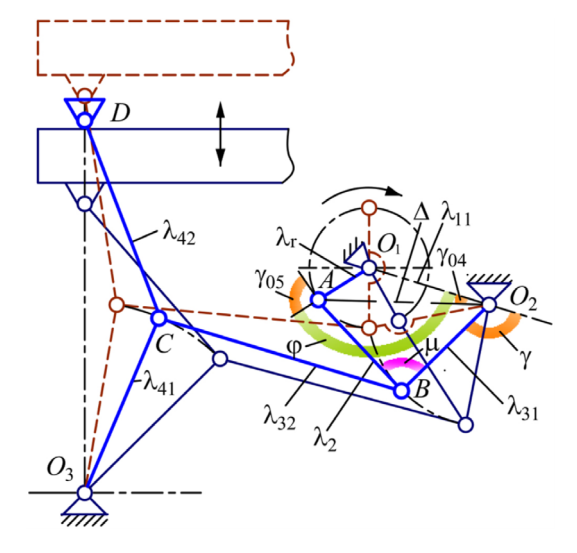
$$\Delta = \sqrt{\lambda_{11}^2 + \lambda_r^2 - 2 \cdot \lambda_r \cdot \lambda_{11} \cdot \cos(\varphi)}$$
 (44)

The angle $\gamma_{_{04}}$ between the diagonal Δ and the interbase distance $\lambda_{_{11}}$:

$$\gamma_{04} = \arccos\left(\frac{\Delta^2 + \lambda_{11}^2 - \lambda_r^2}{2 \cdot \lambda_{11} \cdot \Delta}\right) \tag{45}$$

The angle γ_{os} between the driving crank λ_r and the driving connecting rod λ_s :

$$\gamma_{05} = \arccos\left(\frac{\Delta^2 + \lambda_2^2 - \lambda_{31}^2}{2 \cdot \lambda_2 \cdot \Delta}\right) \tag{46}$$



» **Figure 8:** Scheme for calculating the left contour of the double-wedging mechanism of the pressure plate drive (determination of the angles of the current position of the mechanism)

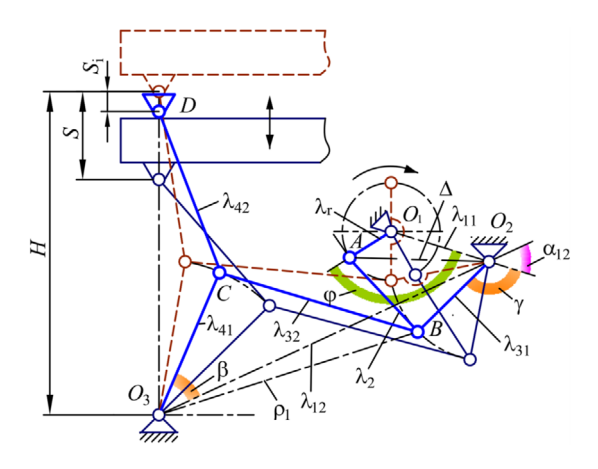
Transmission angle μ between the driven rod λ_2 , and the driving connecting rod λ_3 :

$$\mu = \arccos\left(\frac{\lambda_2^2 + \lambda_{31}^2 - \Delta^2}{2 \cdot \lambda_2 \cdot \lambda_{31}}\right) \tag{47}$$

The inclination angle γ of the driven rod λ_{2} to the interbase distance λ_{3} :

$$\gamma = \mu + \gamma_{04} \pm \gamma_{05} \tag{48}$$

Below is the calculation of kinematic parameters (Fig. 9) for determining the pressure plate's displacement, velocity, and acceleration.



» Figure 9: Scheme for calculation of the left contour of the double wedging mechanism of the pressure plate drive (determination of the current displacement of the pressure plate)

The angle $\alpha_{_{12}}$ between the interbase distances $\lambda_{_{11}}$ and $\lambda_{_{12}}\!\!:$

$$\alpha_{12} = \alpha_1 + \alpha_2 \tag{49}$$

Relative diagonal ρ₁:

$$\rho_{1} = \sqrt{\lambda_{12}^{2} + \lambda_{31}^{2} - 2 \cdot \lambda_{12} \cdot \lambda_{31} \cdot \cos(\pi - \gamma - \alpha_{12})}$$
 (50)

The inclination angle β of the drive rod λ_{a_1} to the interbase distance λ_{i_2} :

$$\beta = \arccos\left(\frac{\lambda_{41}^{2} + \rho_{1}^{2} - \lambda_{32}^{2}}{2 \cdot \lambda_{41} \cdot \rho_{1}}\right)$$

$$\pm \arccos\left(\frac{\lambda_{12}^{2} + \rho_{1}^{2} - \lambda_{31}^{2}}{2 \cdot \lambda_{12} \cdot \rho_{1}}\right)$$
(51)

Relative movement of the pressure plate S_i:

$$s_i = 2 \cdot \lambda_{41} \cdot \sin(\alpha_2 + \beta) - H + S \tag{52}$$

The relative velocity of the pressure plate V:

$$V_{i} = \frac{dS_{i}}{d\varphi} \tag{53}$$

The relative acceleration of the pressure plate a:

$$a_{i} = \frac{dV_{i}}{d\varphi} \tag{54}$$

To get the absolute values of the kinematic parameters of the mechanism, we use dependencies 55, 56, and 57 (S- linear displacement; V – velocity; a – acceleration):

$$S = s_i \cdot [S_{\text{max}}] \tag{55}$$

$$V = V_i \cdot [S_{\text{max}} \cdot \omega_r] \tag{56}$$

$$a = a_i \cdot [S_{\text{max}} \cdot \omega_r^2] \tag{57}$$

where S_{max}=80 mm (3.14961 in) is the absolute maximum linear displacement of the pressure plate, $\omega_r = \pi \cdot n/30$ is the angular velocity of the driving crank, and n=60 rpm is the crankshaft rotation velocity.

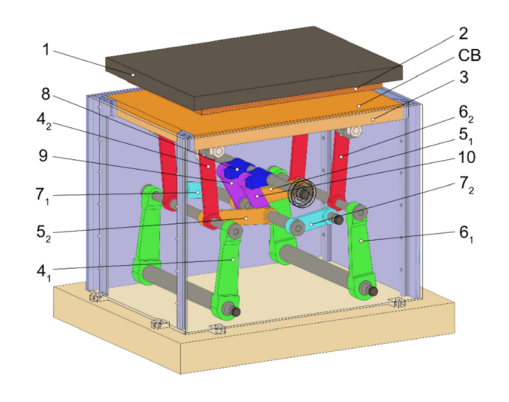
Virtual Experiment of the 3D Model of the Mechanism

The proposed double-wedging mechanism's virtual kinematic analysis was performed in the SolidWorks program based on a 3D model and mechanism operation simulation (Fig. 10).

In the figure, 1 – fixed plate, 2 – die-cutting form, 3 – pressure plate, 4_1 and 6_1 – drive rods, 4_2 and 6_2 – driven connecting rods, 5_1 and 5_2 – power rods, 7_1 and 7_2 – driven rods, 8 – driven crank, 9 and 10 – driving connecting rods. Analytical dependencies were derived below (Table 1).

Table 1Geometric parameters for designing a 3D model of the research double-wedging mechanism

Parameters	Dimension (mm)	Dimension (in)
Total width of mechanism, H	500	19.685
Maximum pressure plate linear displacement, S _{max}	80	3.14961
The horizontal distance between the supports O ₁ and O ₂ , W ₁	125	4.92126
The horizontal distance between the supports O ₁ and O ₃ , W	250	9.84252
The vertical distance between the supports O ₁ and O ₂ , H ₁	45.85	1.80512
Driving crank, pos. 8	62.83	2.4736
Driving connecting rod, pos. 9, 10	182.78	7.196063
Driven rod, pos. 7 ₁ , 7 ₂	126.58	4.98346
Power rod, pos. 5 ₁ , 5 ₂	229	9.01575
Drive rod, pos. 4 ₁ , 6 ₁	250.95	9.8799
Driven connecting rod, pos. 4 ₂ , 6 ₂	250.95	9.8799



» Figure 10: 3D model of the double-wedding mechanism in the drive of the die-cutting press pressure plate

A kinematic analysis of the researched double-wedging mechanism (Fig. 3) was also performed in the SolidWorks program to compare the results of the kinematic analysis of the existing mechanism. The results are obtained in the form of graphs.

Results

According to the results of the geometric synthesis, considering the initial conditions, the relative geometric parameters of the double-wedging mechanism of the pressure plate drive were determined. They are: $\lambda_r = 0.823 - \text{the driving crank size}; \ \lambda_\eta = 1.664 - \text{interbase}$

distance between axes O_1 and O_2 ; λ_{12} = 5.634 – interbase distance between axes O_3 and O_2 ; λ_2 = 1.645 – the length of the connecting rod of the driving circuit; λ_3 = 1.582 – the lever length of the horizontal wedging circuit; λ_3 = 2.862 – the connecting rod length of the horizontal wedging circuit; λ_4 = 3.137 – the lever length of the vertical wedging circuit; λ_4 = 3.137 – the connecting rod length of the vertical wedging circuit. At the same time, the relative maximum linear displacement of the pressure plate was assumed to be equal to S=1, and the main relative basic dimensions were similar to the existing wedging mechanism of the Bobst die-cutting press.

The kinematic parameters calculating results of the wedging and combined double-wedging mechanisms of the pressure plate drive are shown in Fig. 11 and Fig. 12. But Fig. 11a, Fig. 12a, and Fig. 12c show graphical dependences of the double-wedging mechanism kinematic parameters, which were obtained by the analytical method. The solid line (Fig. 11b, c; Fig. 12b, d) shows the graphic results of calculating the kinematic parameters of the double-wedging mechanism obtained by modeling the mechanism's operation using the SolidWorks program. The dashed line (Fig. 11b, c; Fig. 12b, d) shows the graphical dependence of the kinematic parameters for the existing wedging mechanism shown in Fig. 3. Fig. 11c shows graphs of the pressure plate linear displacement during contact with a cardboard blank with a thickness of $h_{CB} = 1 \text{ mm}$ (0.0393701 in) on an enlarged scale.

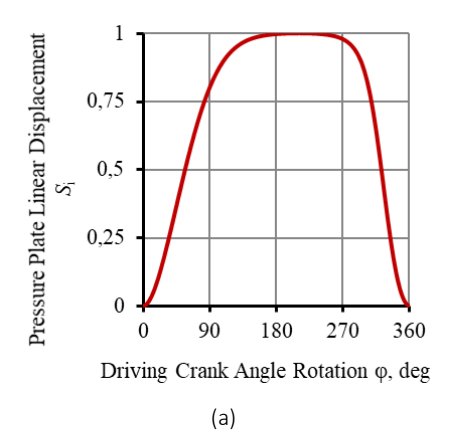
The analysis of linear displacement $S_{\rm p}$ velocity $V_{\rm p}$ and acceleration $\alpha_{\rm l}$ of the double-wedging mechanism according to the derived analytical dependencies was performed in relative values relative to the angle φ (degrees) of the driving crank rotation. When simulating the operation of the wedging and double-wedging mechanisms in the SolidWorks program, kinematic parameters were analyzed in absolute values relative to time t (sec). The absolute linear displacement of the pressure plate was assumed to be equal to $S_{\rm max}$ =80 mm (3.14961 in), as in the existing die-cutting presses of the Bobst company. The number of revolutions of the drive crank was n=60 rpm, and the duration of one pressure plate movement cycle was t=1 sec.

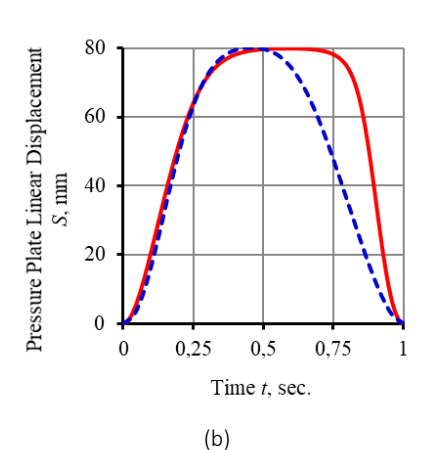
A comparative analysis of graphical dependencies obtained through the analytical method and the double-wedging mechanism simulation in the SolidWorks program demonstrated their complete identity. This confirms the validity of the derived analytical equations for calculating the parameters of the combined double-wedging mechanism of the pressure plate drive.

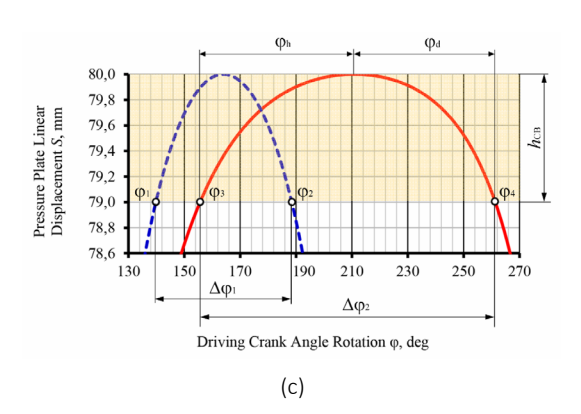
As can be seen from the dependences $S_i = f(\varphi)$ (Fig. 11, a) and S = f(t) (Fig. 11, b) in sections $\varphi = 0^\circ - 140^\circ$ (t = 0 - 0.4 sec.), there is a rapid increase in the displacement of the pressure plate. When approaching the uppermost position, the movement of the pressure plate slows down.

It increases the contact duration of the pressure plate with the cardboard blank of the short circuit and the mold (die-cutting or relief for embossing), which is an essential positive technological point.

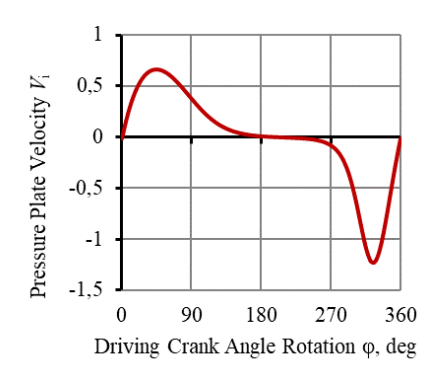
It has a particularly positive effect on the technological operations of relief embossing and creasing, which require long-term contact of the die-cutting mold with the cardboard blank *CB*.

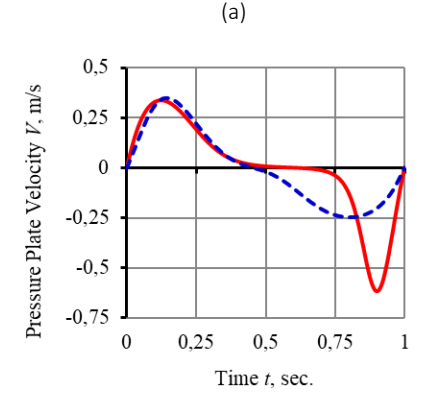


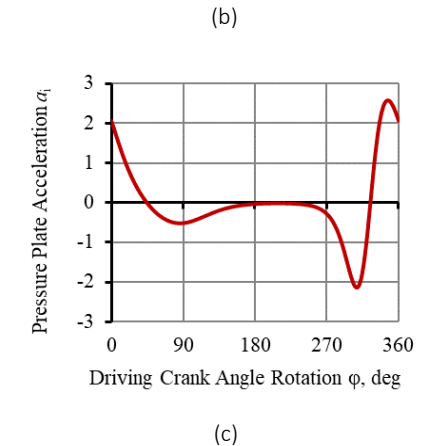


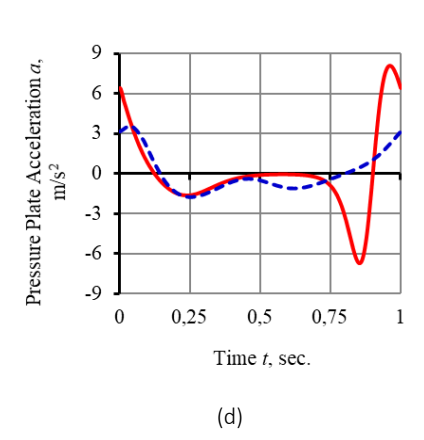


» **Figure 11:** The results of calculating the pressure plate movement of the double-wedging mechanism (solid line) and the existing wedging mechanism (dashed line) obtained by the analytical method (a), modeling in the SolidWorks program (b), the area of the plate movement during contact with the cardboard blank CB (c) of the thickness $h_{\text{CB}} = 1 \text{ mm}$ (0.0393701 in)









» Figure 12: The results of calculating the velocity and acceleration of the pressure plate of the double-wedging mechanism (solid line) and the existing wedging mechanism (dashed line) obtained by the analytical method (a, c) and modeling in the SolidWorks program (b, d)

For example, for cardboard blank *CB* with a thickness of $h_{\rm CB}$ =1 mm (0.0393701 in) (Fig. 11c), the angle of drive crank rotation during the contact of the pressure plate with the cardboard *CB* for the exciting wedging mechanism: $\Delta \phi_1 = \phi_2 - \phi_1 = 188^\circ - 140^\circ = 48^\circ$, for the double-wedging mechanism $\Delta \phi_2 = \phi_4 - \phi_3 = 261^\circ - 156^\circ = 105^\circ$.

As we can see, the proposed double-wedging mechanism ensures that the contact time of the pressure plate with the cardboard blank is 2.18 times longer than the existing wedging mechanism.

An essential point for the proposed double-wedging mechanism is the difference in the pressure plate's working (raising) and idle (lowering) movement during contact with the cardboard CB . So, for cardboard with a thickness of $h_{\rm CB}$ =1 mm (0.0393701 in), the turning angle of the crank when raising the plate is ϕ_h =211°–156°=55°, and when lowering it, ϕ_d =261°–211°=50°. It ensures a longer time of compression deformation of the cardboard and, as a result, the formation of the necessary residual deformation during creasing or relief embossing. The difference in the duration of the working (raising) and idle (lowering) movements of the pressure plate is explained by the combined mechanism of its drive.

Analysis of the velocity of pressure plate linear displacement (Fig. 12a, b, solid line) shows that its relative maximum value during the working stroke is observed at the crank's rotation angle φ =44° and is $V_{\rm max}$ =0.67. At the angle of crank rotation φ =211°, the velocity of the pressure plate changes its direction to the opposite, and until the end of the cycle, its values are negative. During the reverse stroke, the relative maximum negative value of the velocity is equal to $V_{\rm max}$ =-1.23 at the angle of rotation of the crank φ =325°. The corresponding absolute values of the velocity are $V_{\rm max}$ =0.33 m/sec (1.082677 ft/sec) when lifting and $V_{\rm max}$ =-0.62 m/sec (-2.034121 ft/sec) when lowering the plate.

The difference between the maximum velocity of the pressure plate during lifting and lowering is explained by the steeper displacement curve (Fig. 11a, solid line) during its lowering.

Analysis of the dependences of velocity (Fig. 12a, b) and acceleration of the pressure plate (Fig. 12c, d) in the double-wedging mechanism (Fig. 12, solid line) shows that at the peak values of the velocity, the acceleration of the plate is equal to a=0 m/sec² (0 ft/sec²). It observes values of the angle of crank rotation φ =44° and φ =325° for the relative values obtained according to analytical dependencies and at t=0.12 sec and t=0.9 sec for absolute values obtained by modeling in the SolidWorks program. At the same time, the relative maximum acceleration value $a_{\rm imax}$ =2.57 is observed at φ =346°, and the absolute maximum value is $a_{\rm max}$ =8.09 m/sec² (26.5419 ft/sec²) at t=0.96 sec.

A comparative analysis of the velocity and acceleration of the pressure plate for wedging (Fig. 12b, d, dashed line) and double-wedging mechanisms (Fig. 12b, d, solid line) shows the following. The maximum velocity value for both mechanisms when raising the plate is approximately the same. When lowering it for the wedging mechanism, it is 0.53 times smaller (0.33 m/sec (1.0827 ft/sec) and 0.62 m/sec (2.03412 ft/sec), respectively). The maximum value of the pressure plate acceleration in the wedging mechanism is 3.3 m/sec² (10.8268 ft/sec²), and in the double wedging mechanism, it is 8.09 m/sec² (26.5419 ft/sec²). It is known that inertial forces in a die-cutting press are not decisive, unlike technological ones. Therefore, an increase in acceleration, and accordingly, inertial forces, by 2.4 times will not significantly affect the press drive.

Conclusion

Scientific research on improving die-cutting presses has been critically analyzed. No information exists on the study of the mechanisms of the pressure plate movement with an increased duration of contact of the die-cutting tools with the cardboard. This information is crucial when performing technological operations such as creasing and relief embossing.

A scheme of the double wedging mechanism of its drive is proposed to increase the pressure plate's contact period with the cardboard blank. The proposed mechanism was geometrically synthesized, and its relative geometric parameters were determined. At the same time, the main basic dimensions were assumed to be similar to those of the existing wedging mechanism of the Bobst die-cutting press.

A methodology for calculating the kinematic parameters of the combined double-wedging mechanism of the pressure plate drive has been developed. It involves a "reverse" calculation, in which the "unit" is taken as the relative linear movement S=1 of the driven link (the pressure plate), which corresponds to its movement $(S_{mw}=80 \text{ mm}, 3.14961 \text{ in})$ in Bobst's die-cutting presses.

Mathematical models were created, which made it possible to calculate the relative kinematic parameters of the combined double wedging mechanism of the pressure plate drive. According to the results, it was established that the change in the movement of the pressure plate ensures its long-term contact with the cardboard blank. For example, for cardboard with a thickness of 1 mm, the plate's contact period with the cardboard corresponds to the rotation angle of the drive crank of 105°. It is 29% of the total movement period of the pressure plate. The change in the direction of the velocity from positive to negative at the angle of rotation of the crank φ =211° proves that the period of raising the plate is greater than the period of its lowering.

A comparative analysis of the results of analytical studies with the results of a virtual experiment of the existing wedging and the proposed double-wedging mechanisms in the SolidWorks program was performed. According to his results, it was established that for the existing mechanism, the contact of the pressure plate with the cardboard blank occurs during the angle of rotation of the crank, which is equal to $\varphi\text{--}48^\circ$. It accounts for 13.3% of the total period of plate movement, which is 0.46 times less than for the case of the double-wedging mechanism.

Thus, a combined double-wedging mechanism provides twice as prolonged contact between the pressure plate and the cardboard blank. It creates better prerequisites for obtaining the technologically necessary residual deformation during the creasing and relief embossing of cardboard blanks.

Funding

This research did not receive any specific grant from funding agencies in the public, commercial, or not-for-profit sectors.

References

- Emblem, A. & Emblem H. (2012) *Packaging tech*nology Fundamentals, Materials and Processes. Oxford, Woodhead Publishing.
- Khvedchyn, Y. Y. & Zelenyi, V. V. (2014) Analysis of The Mechanisms of Press in Die-cutting Automat. *Scientific Papers*. 4 (49), 21-30.
- Kirwan, M. J. (2013) *Handbook of Paper and Paper-board Packaging Technology.* Oxford, John Wiley & Sons. Available from: doi: 10.1002/9781118470930
- Kuznetsov, V. O. Rehei, I. I. & Vlakh, V. V. (2017) Modification of a drive mechanism of a press plate in a die-cutting press. *Printing and Publishing*. 1 (73), 56-62.

- Kuznetsov, V. O., Kolomiets, A. B. & Dmitraschuk, V. S. (2012) Parametric Researches of the Press Plate Drive in Die-cutting Automat. *Packaging*. 6, 31-34.
- Lin, W., Zhou, C. & Huang, W. (2015) Optimum design for mechanical Structures and Material Properties of the dual-elbow-bar mechanism. *Advances in Materials Science and Engineering*. 2015. Available from: doi: 10.1155/2015/724171
- Pasika, V. R. & Vlakh, V. V. (2016) Kinematic synthesis of die-cutting press mechanism with equality of forward and reverse moves. *Printing and Publishing*. 1 (71), 129-139.
- Poliudov, O. M. (2005) *Mechanics of printing and packaging machines*. Lviv, Ukrainian Academy of Printing.
- Rehei, I. I., Vlakh, V. V., Knysh, O. M. & Mlynko, O. I. (2022) Complex analysis of the pressure plate drive mechanisms functioning in die-cutting presses. *Printing and Publishing*. 2 (84), 88–98. Available from: doi: 10.32403/0554-4866-2022-2-84-88-98
- Rehei, I., Vlakh, V., Knysh, O., Knysh, R. & Mlynko, O. (2023) Combined double crank wedging drive mechanisms of the press plate used in die-cutting press: synthesis, kinematic and functional. *Academic* journal of manufacturing engineering. 3 (21), 53-60.
- Rehei, I. I. (2011) Consumer Cardboard Packaging: Materials, Design Manufacturing Equipment. Lviv, Ukrainian Academy of Printing.
- Shakhbazov, Y. O., Cheterbuh, O. Y., Shyrokov, V. V. & Palamar, O. O. (2020) The drive mechanism of a pressure plate of a flat die-cutting press. *Printing and Publishing*. 1 (79), 112-120. Available from: doi: 10.32403/0554-4866-2020-1-79-112-120
- Vlakh, V. & Pasika, V. (2016) Automated synthesis of mechanism of press of diecutting machine. *Technological Complexes*. 1 (13), 57-63.
- Wang, J., Chen, X. & Li, Y. (2023) Structure Design and Optimization Algorithm of a Lightweight Drive Rod for Precision Die-Cutting Machine. *Applied Sciences*. 13 (7). Available from: doi: 10.3390/app13074211



© 2025 Authors. Published by the University of Novi Sad, Faculty of Technical Sciences, Department of Graphic Engineering and Design. This article is an open access article distributed under the terms and conditions of the Creative Commons Attribution license 4.0 Serbia (https://creativecommons.org/licenses/by/4.0/deed.en).